Proceedings of ASME Turbo Expo 2011
GT2011
June 6-10, 2011, Vancouver, British Columbia, Canada

GT2011-46192

150 KW CLASS TWO-STAGE RADIAL INFLOW CONDENSING STEAM TURBINE SYSTEM

Kazutaka Hayashi **Hiroyuki Shiraiwa** **Hiroyuki Yamada**
Hitachi Engineering & Services Co. Ltd.
1-15-1, Higashiohnuma-cho, Hitachi, Ibaraki, Japan

Susumu Nakano
Energy and Environmental Systems Laboratory, Hitachi, Ltd.
3-1-1, Saiwai-cho, Hitachi, Ibaraki, Japan

Kuniyoshi Tsubouchi
Formerly with Power & Industrial Systems R & D Laboratory, Hitachi, Ltd.
3-1-1,Saiwai-cho Hitachi, Ibaraki, Japan

ABSTRACT
A prototype machine for a 150 kW class two-stage radial inflow condensing steam turbine system has been constructed. This turbine system was proposed for use in the bottoming cycle for 2.4 MW class gas engine systems, increasing the total electrical efficiency of the system by more than 2%. The gross power output of the prototype machine on the generator end was 150kW, and the net power output on the grid end which includes electrical consumption of the auxiliaries was 135kW. Then, the total electrical efficiency of the system was increased from 41.6% to 43.9%. The two-stage inflow condensing turbine system was applied to increase output power under the supplied steam conditions from the exhaust heat of the gas engines. This is the first application of the two-stage condensing turbine system for radial inflow steam turbines. The blade profiles of both high- and low-pressure turbines were designed with the consideration that the thrust does not exceed 300 N at the rated rotational speed. Load tests were carried out to demonstrate the performance of the prototype machine and stable output of 150 kW on the generator end was obtained at the rated rotational speed of 51,000 rpm. Measurement results showed that adiabatic efficiency of the high-pressure turbine was less than the design value, and that of the low-pressure turbine was about 80% which was almost the same as the design value. Thrust acting on the generator rotor at the rated output power was lower than 300 N. Despite a lack of high-pressure turbine efficiency, total thermal efficiency was 10.5% and this value would be enough to improve the total thermal efficiency of a distributed power system combined with this turbine system.

NOMENCLATURE
ΔH_{is}: isentropic heat drop (J/kg)
ΔH_{av}: available heat drop (J/kg)
h: specific enthalpy (J/kg)
v_0: isentropic velocity (m/s) ($v_0^2=2\Delta H_{is}$)
w: circumferential velocity (m/s)
y: wetness (-)
η: efficiency (-)

Subscripts
ex: exit
in: inlet
is: isentropic
sat: saturated steam
w: saturated water

INTRODUCTION
Reciprocating engines like gas engines are widely used in small to large sizes as distributed power generators. These reciprocating engines have electrical efficiencies around 40 %. Though total efficiencies for co-generation systems that produce electricity and steam reach above 82 %, it is necessary to produce much more electricity rather than steam from the generator exhaust heat. Thus, some designers of systems have attempted to obtain electricity from waste energy of gas turbines and gas engines or from other heat sources, such as geothermal. The organic Rankine cycle (ORC) is often applied to these systems because it is considered an effective way to produce electricity from such low grade heat [1, 2]. The

working fluid of an ORC should not leak into the environment and it should have low environmental impact. Then there is interest in getting an alternative to organic working fluids based on considerations for efficiency, economy, and possible environmental impact.

In this study, the steam Rankine cycle is proposed for application as the bottoming cycle for reciprocating engine systems to increase electric output power. Radial inflow steam turbine systems can be placed directly on existing distributed power generators that are equipped with a heat recovery steam generator. As steam is the working fluid for the generator, it is easy to handle without extra consideration for the environment. Owners of the distributed power generators can easily chose between electricity and steam.

The main aims are for the system to produce high quality electricity in a highly efficient way from saturated steam with a pressure of less than 1.0 MPa generated by exhaust heat of gas engines and to minimize any environment impact caused by using the system. The design specifies that saturated steam (0.78 MPa; flow rate, 0.53 kg/s) is generated by exhaust heat from a 2.4 MW gas engine and is expanded through two-stage radial inflow turbines (total pressure ratio, 16). When the gross power output on the generator end is 150kW, the power conversion system loss is about 7kW and electrical consumption of the auxiliaries (such as vacuum and circulation water pumps, etc.) is about 8kW. Then, output electrical power of 135 kW is produced on the grid end. This electrical power increases the efficiency of the gas engine from 41.6 % to 43.9 %. To simplify the main structure of the turbine system and to reduce mechanical friction loss, a permanent magnet rotor with water-lubricated bearings [3] is applied as a generator rotor. Application of the water-lubricated bearings means that the system completely eliminates oil supply units and is very environmentally friendly.

Rated load tests to confirm the design concepts of the prototype machine [4] have almost been completed and stable power of 150 kW on the generator end was obtained. Operation method of the turbine system, measurement methods, and test results are shown in this paper.

TOTAL SYSTEM

Figure 1 is a system diagram of the radial inflow steam turbine used in the present study. A two-stage condensing turbine system is applied to increase output power under the supplied steam conditions from exhaust heat of gas engines. To reduce mechanical losses, a permanent magnet generator rotor is applied that has turbine rotors in a common shaft. Electric power produced by the generator is converted from high frequency on the generator end to commercial frequency on the grid end by the power conversion system. This type of generator rotor, which has the turbine rotor placed on both ends of the generator rotor in a common shaft, will often have to pass critical speeds of rotor vibration. Water-lubricated bearings that support the rotor are adopted for two reasons: one is to pass the critical speeds of rotor vibration easily, and the other is to reduce bearing loss for this high-speed rotor. A combined bearing that has both journal and thrust bearings is set on the high-pressure turbine side, and a journal bearing is set on the low-pressure turbine side.

The system has four subsystems providing steam, water, cooling air, and exhaust vacuum. The steam supply line is drawn in red in Figure 1. Saturated steam from a boiler is supplied to the high-pressure turbine through a stop valve and a flow control valve. After passing through the high-pressure turbine, condensed water included in wet steam is eliminated at the drain separator, and the steam is supplied to the low-pressure turbine as saturated steam. The exhaust steam is then sent to the condenser and condensed into water. The condensed water is pooled in the hot well, which is kept at a certain vacuum pressure by the vacuum pump, and is discharged to the outside afterward. The water supply line in blue in Figure 1 is composed of the circulation water tank, the circulation pump, and the heat exchanger. Water pumped up by the circulation pump provides cooling as it goes through the exchanger and is sent to the bearings, the cooling jacket of the generator, and the power conversion system. Lubricating water of the bearings and cooling water of the generator and power conversion system are returned to the circulation water tank. The air supply line is in light green in Figure 1. Cooling air is supplied to the gap between the inner surface of the stator and the outer surface of the rotor and is exhausted to the outside of the generator. Seal air is supplied to both sides of each bearing to prevent incursion of the splashed water from lubricant water. Pressure at the back of the low-pressure turbine rotor becomes less than the atmospheric pressure. Steam is also introduced from the steam supply line to be used as seal steam to prevent seal air or ambient air from entering the back of the low-pressure turbine rotor and mixing with the main flow steam of the turbine.

Operation conditions like pressure, temperature, and mass flow rate for several portions of the system at the rated rotational speed are given in Figure 1. These values are determined as the final specifications for the system design. Utilizing water for lubrication means that the oil supply unit is completely eliminated from this turbine system. This contributes to reductions in auxiliary power and environmental impact.

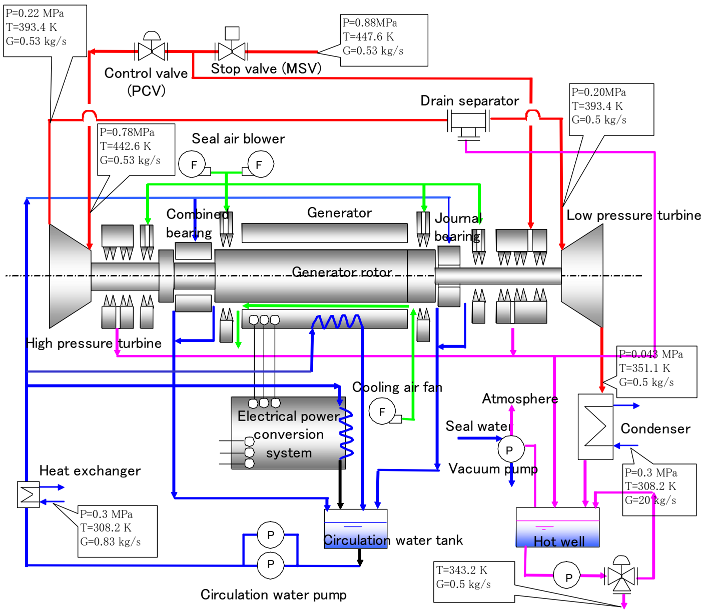

Fig. 1 System diagram

DESIGN SPECIFICATIONS

Turbine design

Profiles of the turbine rotors are designed by a conventional method for radial turbines that includes some iteration procedures from one-dimensional (1D) aerodynamic design [4] [5], three-dimensional (3D) blade profile design [6] to three-dimensional (3D) viscous flow analysis [6] [7]. Before making the profiles designs for turbines, pre-calculations to determine the preliminary specifications like pressure ratios of high- and low-pressure turbines, rotational speeds, turbine rotor diameters are carried out according to Balje [5], and thrust acting on the turbine rotors is also calculated using equations shown in Nakano et al. [4]. As one of the main concepts is to simplify the rotor system, balance pistons are not applied to cancel the thrust. Better selection for both diameters of the high- and low-pressure turbines requires high efficiency and less thrust.

Total pressure ratio from the high-pressure stage to the low-pressure stage is set at 16 on the basis of a pressure ratio of 4 for a single stage turbine [8]. Figure 2 shows the adiabatic efficiency of the high- and the low-pressure turbines at three combinations of pressure ratio of each turbine. The rotational speed which provides the maximum efficiency of the high-pressure turbine is about 66000rpm. And that for the low-pressure turbine is about 37000rpm. Considering the combined efficiency of both turbines, the pressure ratios of 3.5 for the high-pressure turbine and 4.6 for the low-pressure turbine are selected. These pressure ratios are also selected with consideration of the thrust which does not exceed 300 N at the rated rotational speed.

Figure 3 plots the total turbine power and the total adiabatic efficiency against the rotational speed. The power limit of the generator is also shown. This graph shows the best efficiency point is 46000rpm. But, the total turbine power at this rotation speed exceeds the power limit of the generator. Thereby, the rated rotational speed is set as 51000rpm, which is the rated rotational speed of the generator. Though the power at 51000rpm is slightly lower than the best point, it has some safety margin against the power limit of the generator.

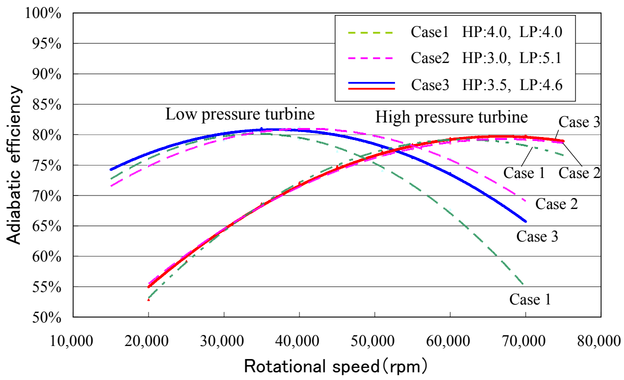

Fig. 2 Adiabatic efficiency of each turbine
- preliminary specifications design -

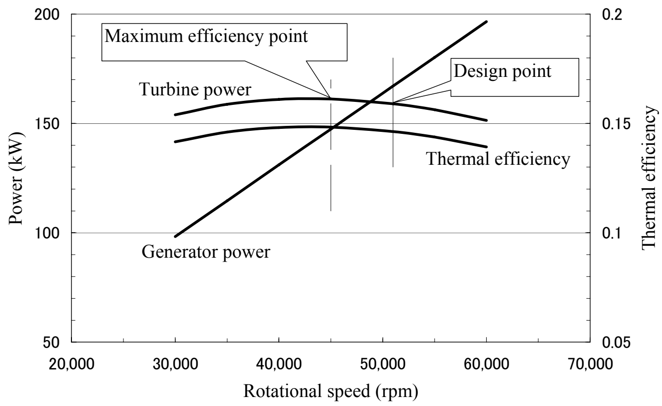

Fig. 3 Total turbine system performance
- preliminary specifications design -

As mentioned before, the details of turbine rotors were determined to use some iteration procedures from 1D aerodynamic to 3D viscous analysis. Specifications and main results of detailed blade profile design are summarized in Table 1. Figure 4 is a photograph of the high-pressure turbine rotor, and Figure 5 is one of the low-pressure turbine rotor. The adiabatic efficiency of the high-pressure turbine is 76.9% and that of the low-pressure turbine is 77.9%.

Table 1 Specifications and some design results

Items		Unit	High-pressure turbine	Low-pressure turbine
Conditions	Inlet pressure	MPa	0.78	0.2
	Inlet temperature	K	442.6	393.4
	Mass flow rate	kg/s	0.53	0.5
	Pressure ratio	-	3.5	4.6
	Adiabatic efficiency	%	76.9	77.9
Design value	Rated rotational speed	rpm	51000	51000
	Diameter	m	0.154	0.184
	Circumferential velocity	m/s	411	491
	Blade number	-	11	14
CFD results	Reaction	-	0.46	0.43
	Wetness	%	6	6.5

Fig. 4 Photograph of the high-pressure turbine rotor

Fig. 5 Photograph of the low-pressure turbine rotor

Water-Lubricated Bearings

As shown in Figure 1, the rotor is supported by two water-lubricated bearings on each side of the permanent magnet rotor. One is the journal bearing located on the side of the low-pressure turbine, and the other is the journal and thrust combined bearing located on the other side of the permanent magnet rotor, which is next to the high-pressure turbine. Water-lubricated bearings are applied to simplify the radial inflow steam turbine system. The damping effect is larger than that for air bearings, which can surpass the critical speed of rotor vibrations and has a bearing loss less than that for oil bearings. Thus, utilizing water contributes to increased total efficiency and electrical output of the turbine system.

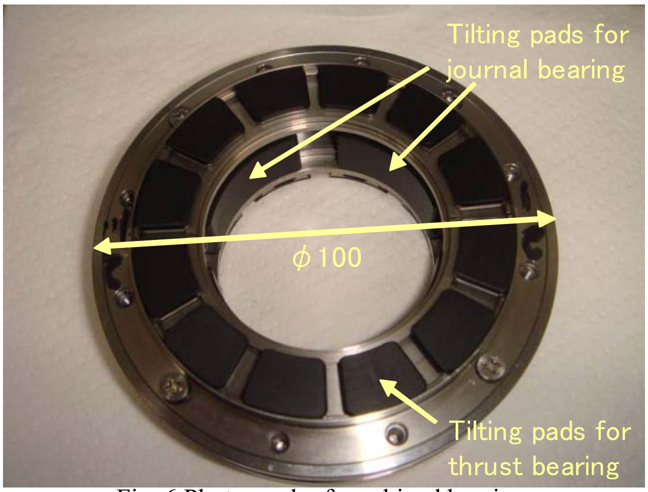

Fig. 6 Photograph of combined bearing

The journal and thrust combined bearing has 12 tilting pads in the thrust bearing, and four tilting pads in the journal bearing. The journal bearing located on the low-pressure turbine side also has four tilting pads. Poly-Ether-Ether-Ketone (PEEK) plastic is used as contact surface material for both journal and thrust bearings because of good wear resistance, good heat resistance, low friction coefficient, and sufficient strength as required for bearings that sustain a high-speed rotor. Figure 6 is a photograph of the combined bearing.

The journal bearing loss on the high-pressure turbine side was estimated by Nakano et al. [4] to be about 3.7kW at the rated rotational speed of 51,000rpm and that on the low-pressure turbine side was about 1.8kW. A 20% increase of the diameter of the journal bearing doubled the bearing loss. Nakano et al. [4] also found that the thrust bearing loss differed according to the thrust load. About 1.8kW loss was estimated to be caused by a thrust load of 300N. Figure 7 shows results of the calculated thrust bearing losses. Furthermore, the thrust bearing loss with the churning loss, which is caused by the friction shear force of the lubricant water outside the bearing pads, became about 3.0 kW on the thrust bearing.

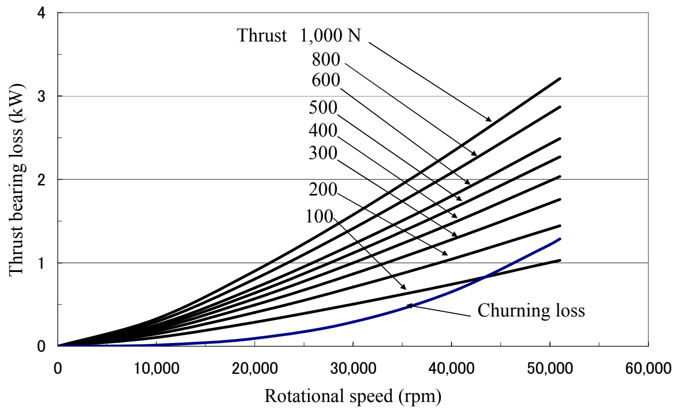

Fig. 7 Calculated thrust bearing losses

CONFIGURATION OF MAIN COMPONENTS

A prototype turbine system has been constructed. Figure 8 shows the packed assembly of the turbine system. The electric conversion system is not placed in the packaged assembly. Outside dimensions of the package are as follows: 3.0 m long, 1.3 m wide and 3.3 m high. As the condenser and drain separator are used in commercial products, those volumes are not optimized for the packaged system. Optimizing the auxiliaries will provide a more compact package.

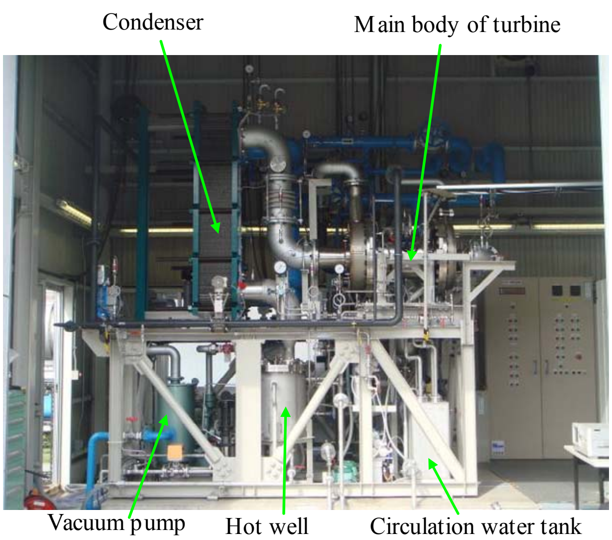

Fig. 8 Configuration of packaged turbine system

MEASUREMENT METHOD

Turbine performance

The generating power is measured at two points. The first is the power on the generator end, and the second is that on the grid end. Efficiency of the power conversion system is measured as the ratio of power output on the grid end to that on the generator end.

For the evaluation of the turbine performance, the temperature and the pressure at the inlet and outlet of both high- and low-pressure turbines, and the flow rates at the inlet of the both turbines are measured. Semiconductor-type sensors are used for pressure measurement, K-type thermocouples for temperature measurement, and the differential pressure type flow meter for flow rate measurement.

The adiabatic efficiency is given by Eq.(1). The specific enthalpy at the inlet of the turbine is calculated from the total temperature and the total pressure, which are measured. Specific enthalpy at the outlet of the turbine is given by Eq. (2). Steam expands from the saturated condition to the wet condition. Specific enthalpy is expressed by summation of specific enthalpies of saturated steam and of saturated water using wetness. So, the wetness of the steam at the outlet of the turbine is necessary to calculate the specific enthalpy.

$$\eta_{ad} = \frac{\Delta H_{av}}{\Delta H_{is}} = \frac{h_{in} - h_{ex}}{h_{in} - h_{ex,is}} \tag{1}$$

$$h_{ex} = h_{ex,sat}(1 - y) + h_{ex,w} y \tag{2}$$

The wetness at the high-pressure turbine can be calculated by measuring the amount of condensed water discharged by the drain separator. As for the low-pressure turbine, the amount of condensed water at the outlet of the turbine cannot be measured. Therefore, the wetness is measured with a steam wetness measurement probe [9]. This measurement method is summarized in the next section.

Optical measurement for wetness

The measurement method for wetness is based on Mie light-scattering theory, and the measurement system was developed by EPRI [9]. The measurement system consists of a probe and an assembly consisting of a light source and spectrophotometer, which are attached to the traverse tube, and power supply module. Figure 9 shows the complete system and Figure 10 is a photograph of the probe head. The probe head contains a slot through which the steam flows, and it measures the characteristics of scattered light which is produced by the suspended water droplets. The steam in the slot is exposed to a collimated beam of light which is projected orthogonal to the direction of steam flow. Spectral analysis reveals light extinction characteristics that can form the basis for calculating physical parameters of the water droplet suspension, such as size distribution and concentration.

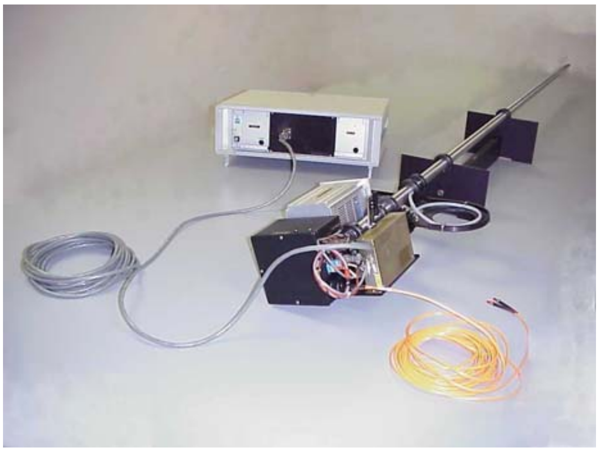

Fig. 9 Photograph of the optical measurement system for wetness

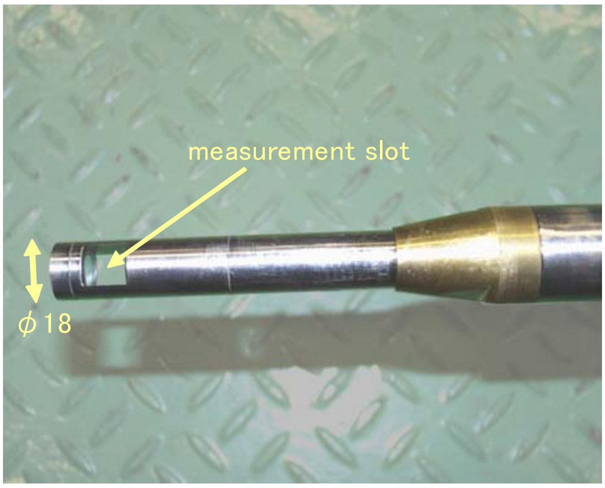

Fig. 10 Photograph of the probe head

Thrust

The thrust load acting on the generator rotor is estimated by summing up the steam pressure on two sides of the high- and low-pressure turbines. The thrust load can be estimated when the pressures acting on the hub faces and the back sides of each turbine are measured. This is simplified when the static pressure of both the turbine inlet and outlet and the root of the back surface of the turbines can be measured [3]. On the other hand, all bearing losses except for thrust, which include friction loss generated by lubricant like churning loss, depend on the rotational speed, not on load. By taking note of the rated rotational speed, bearing loss, which is caused by change of load, is governed by thrust. Temperature rises of lubricant through both the load side and anti-load side of the combined bearing are measured. When the distribution rate of lubricant-water for the load side of the combined bearing is found, thrust bearing loss can be calculated. Based on the results for a similar type of turbine [3], the distribution rate of lubricant water is assumed to be 0.4 - 0.5. Bearing loss measured by temperature rise of the lubricant and the calculated result, which is shown in Figure 7 are compared, and thrust can be deduced.

OPERATION PATTERN

Figure 11 shows the operation pattern of the prototype machine. To be ready for turning of the generator rotor, the circulation water system and the cooling air supply system start up first. Then, the vacuum pump starts up and the pressure in the steam line is kept at low pressure. After the flow rate and the pressure of the circulation water and the cooling air are confirmed to be the specified values, the generator rotor starts up.

In the first step of the operation, the generator rotor is driven as a motor getting its power from the grid. When the rotation speed reaches 6000rpm, the steam pressure control valve (PCV) opens a little and steam is supplied to the system for warming-up. With this steam supply, power-generating operation begins. The rotation speed is kept at 6000rpm during warming-up. Next, the rotation speed increases to the rated value of 51000rpm with constant acceleration. The PCV opens gradually while the rotation speed rises. Then, keeping the speed at 51000rpm, the PCV opens further until the generator power reaches 150kW.

In the stop operation, conversely, the PCV closes gradually until the generator power reaches 10kW, keeping the rotation speed of 51000rpm. Then, the rotation speed drops to 36000rpm with the PCV closing at a constant rate. After reaching 36000rpm, the PCV and the main stop valve (MSV) completely close. Then, electric power supplied by the power conversion system is cut off and the rotation speed decreases to 0rpm by free-running. After 15 minutes of turning operation for cooling, the auxiliary power supplies for the circulation water system and cooling air system stop.

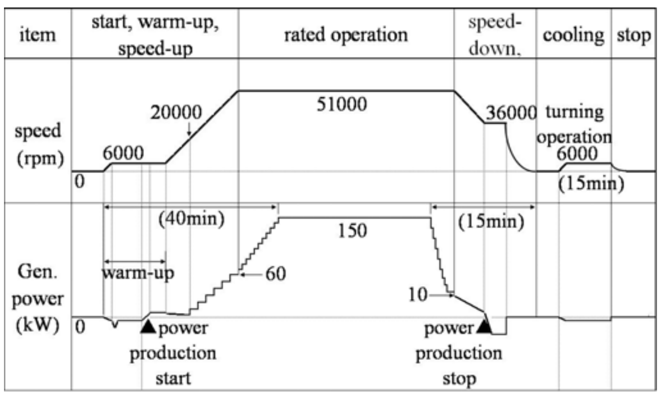

Fig. 11 Operation pattern of the prototype machine

TEST RESULTS

Turbine system performance

Figure 12 is the results at the start-up. After 15 minutes of warming-up operation, the PCV gradually opens and the steam pressure, steam flow rate, the power output increase accordingly. When the rotation speed reaches 51000rpm, the generator power is about 60kW. The PCV continues to open and the generator power reaches 150kW at 38 minutes after the start-up.

Figure 13 is the results at the shutdown. The steam pressure, the flow rate and the generator power decreased gradually as the PCV is closed to 13.5%. Then, the rotation speed drops to 36000rpm and the PCV is closed completely. The shutdown operation takes 12 minutes.

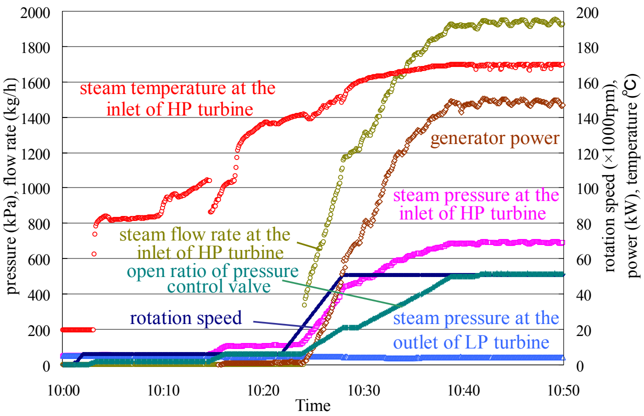

Fig. 12 Test results at the start-up

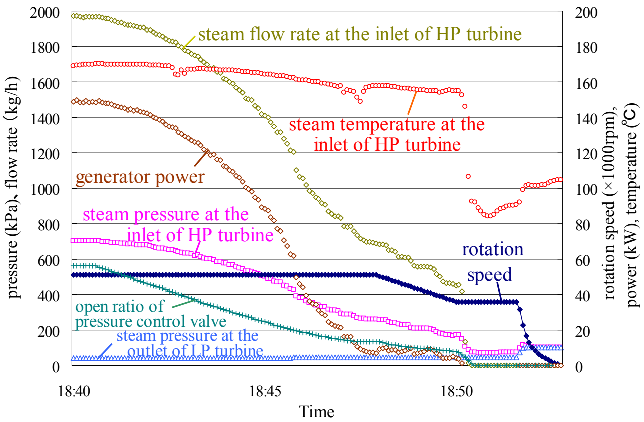

Fig. 13 Test results at the shutdown

Figures14 and 15 show the test results of 150kW load test for 8 hours. After the generator power reaches 150kW, each measured result shows good stability. The generator power is kept at 150kW during the test. The steam temperature at the inlet of high pressure turbine is 170℃ and almost the same as the design value. However, the steam pressure at the inlet of high-pressure turbine is about 700kPa and 80kPa lower than the design value. Meanwhile, the steam pressure and temperature at the inlet of the low-pressure turbine are near the design value, 180kPa and 118.5℃.

The average efficiency of the power conversion system is 96.7%.This is better than the design value of 95%.

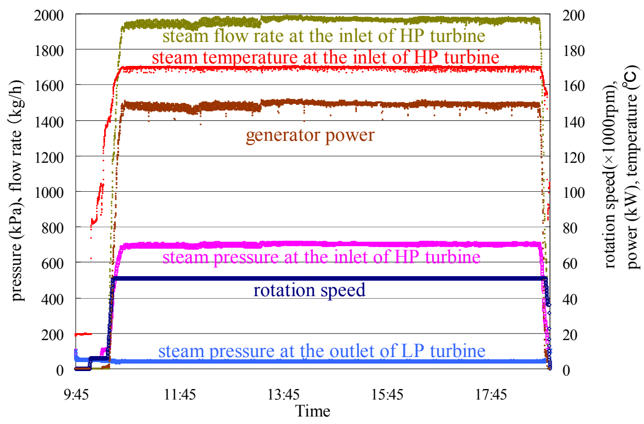

Fig. 14 Test results of temperature, pressure and flow rate for operation of 8 hours

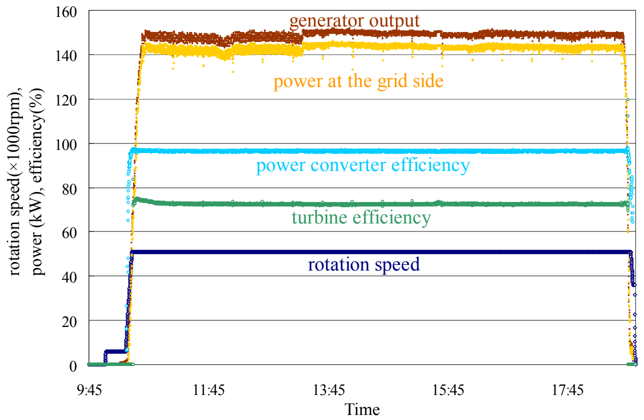

Fig. 15 Test results of output power and efficiencies for operation of 8 hours

Turbine efficiency

Figure 16 shows the adiabatic efficiencies of the turbines plotted against the velocity ratio which is expressed by the ratio of circumferential velocity to isentropic velocity ($v_0^2=2\Delta H_{is}$). The two curves are an approximate correction curve for turbine efficiency which is deduced from the existing characteristic curves for the relationships between efficiency, pressure ratio, and velocity ratio [5]. As for the low-pressure turbine, the measured efficiencies are around 80% and better than the design value of 77.9%. On the other hand, measured turbine efficiencies of the high-pressure turbine are around 55 %. These are significantly lower than the design efficiency of 76.9%. The reason for this 20% lack of efficiency is considered to be the increase of the gap between the nozzle tip and the casing, caused by lack of the nozzle casing stiffness. The steam pressure at the inlet of the high-pressure turbine is lower than the design value, and the steam flow rate at the inlet of the high-pressure turbine is larger than the design value. So, there is some steam leakage at the nozzle tip, and the efficiency of the high-pressure turbine is lower than expected.

The design and the measured wetnesses are shown in Table 2. Compared with the design values, measured values are lower. Especially, wetness of the high-pressure turbine is about half of the design value. The insufficient expansion in the high-pressure turbine is also shown in the comparison between the CFD results and measurements of wetness in Table 2. The 20% lack of efficiency can be mitigated by minimizing the nozzle tip gap.

Figure 17 is the diagram of specific entropy and specific enthalpy of the total system. The adiabatic efficiencies of each turbine are calculated from available heat drop based on the measured wetness. Efficiency of the high-pressure turbine is 58 % which does not reach the design efficiency of 77%. The efficiency of the low pressure turbine is 80% and it is better than the design value of 78%. The total adiabatic efficiency of the turbines is 72.1% on average, which is 6.9% lower than the design value. As a result, the total thermal efficiency of the turbine system cannot reach 15 % which is expected in Fig. 3. Though the total thermal efficiency is 10.5%, this value is enough to improve the total thermal efficiency of a distributed power system when combined with this turbine system to utilize exhaust energy.

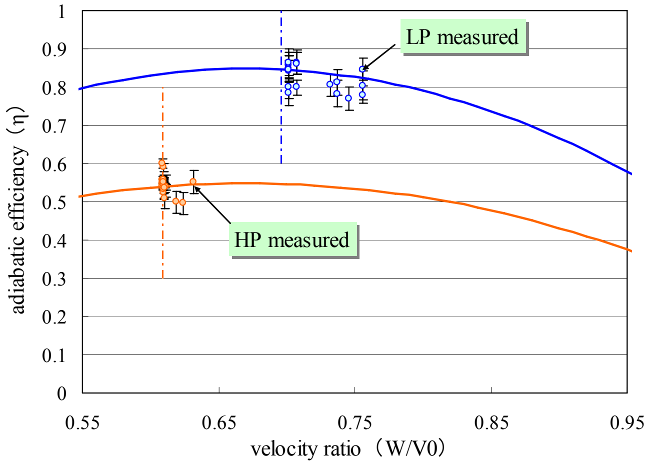

Fig. 16 Relationship between turbine efficiency and velocity ratio

Table 2 Wetness

	CFD results	Measurements
High-pressure turbine	5.99%	2.32±0.26%
Low-pressure turbine	6.50%	5.41±0.49%

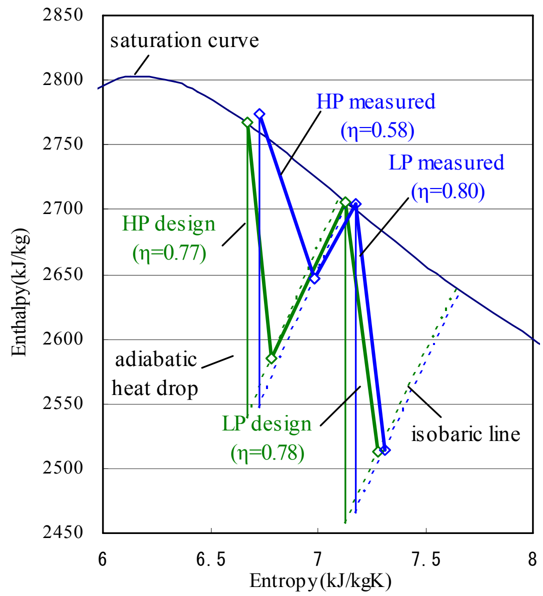

Fig. 17 Enthalpy - entropy diagram of the turbines

Thrust

Figure 18 shows the temperature rise of the bearing lubricant-water. The temperature rise of the combined bearing is 27 ℃ at the 150kW output operation. This is about 10 ℃ higher than that of the journal bearing because of the thrust load and the difference of the bearing diameter. The temperature rise of the combined bearing includes journal bearing loss, thrust bearing loss, churning loss, and friction loss generated by moving the lubricant-water on the surface of the thrust collar. As mentioned before, all bearing losses except for thrust depend on the rotational speed, not on load. After the rotational speed reaches the rated rotational speed, the temperature rise of journal bearing lubricant-water remains constant when the generator output power increases. The temperature rise of the combined bearing lubricant-water increases slightly when the generator power increases from 120 kW to 150 kW. The temperature rises of lubricant through both the load side and anti-load side of the combined bearing are measured. They are plotted in Figure 19. When the temperature difference between the temperature rises of the load side and that of the anti-load side is small, thrust load is assumed to be small too. The temperature difference is caused by thrust load. The temperature difference reaches the maximum at slightly lower point than the output power of 150kW. The lubricant water flow rate is 0.13 kg/s, If the distributed rate of the lubricant water is taken as 0.5, thrust bearing loss will be 1.8 kW. When the distributed rate is 0.4, it will be about 1.5 kW. Comparing these bearing losses to calculated values shown in Figure 7, the maximum thrust at that point is around 300 N. At the output power of 150kW, the temperature difference between the temperature rises of the load side and that of the anti-load side is about 4 ℃, the thrust is lower than 200 N. One of the rotor design concepts is that thrust becomes lower than 300 N because the generator rotor can be simplified without any additional devices, like a balance piston which cancels thrust. Experimental results show that the generator rotor can realize the design concept.

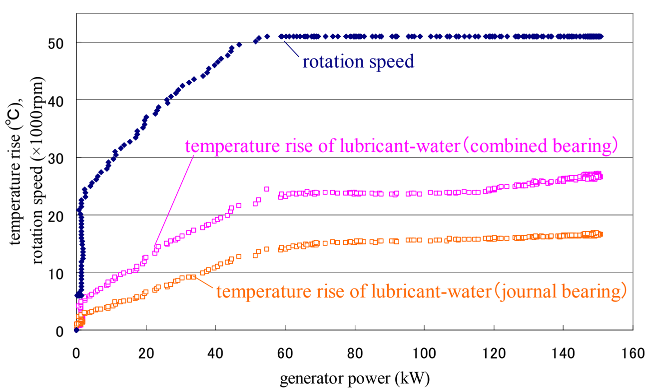

Fig. 18 The temperature rise of lubricant-water

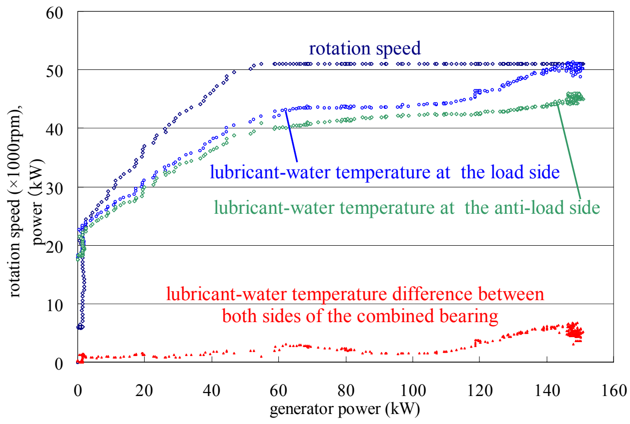

Fig. 19 Comparison temperature rise of lubricant-water through load side with that through anti-load side

CONCLUSION

A 150 kW class two-stage condensing turbine system was proposed to improve the power efficiency of distributed power systems like gas or diesel engine systems. The blade profiles of both turbines were designed with consideration of the thrust which does not exceed 300 N at the rated rotational speed. To reduce mechanical losses, a permanent magnet generator rotor which was composed of turbine rotors in a common shaft supported by the two water-lubricated bearings was applied.

A prototype machine was constructed and its load tests were carried out to demonstrate its performances. This was the first application of radial inflow steam turbines to a two-stage condensing turbine system, and stable output of 150 kW was obtained at rated rotational speed of 51,000 rpm.

Measurement results showed that the total adiabatic efficiency of the turbine was 72.1%, and total thermal efficiency of the prototype turbine system was 10.5%. Thrust acting on the generator rotor at the output power of 150kW was lower than 300 N. These values were enough to improve the total thermal efficiency of distributed power systems.

ACKNOWLEDGMENTS

The authors wish to express their thanks to Dr. Kishibe and Mr. Yagi of Hitachi, Ltd. Energy and Environmental Systems Laboratory for their efforts in the turbine design, to Mr. Inoue and Dr. Yamaguchi of Hitachi, Ltd. Mechanical Engineering Research Laboratory for the bearing and the rotor vibration design, to Dr. Hayasaka of Hitachi, Ltd. Hitachi Research Laboratory for the structure design, to Mr. Kobayashi of Hitachi Engineering & Services Co. Ltd. for the manufacturing the electric conversion system, and to Mr. Kido of Hitachi Engineering & Services Co. Ltd. for assistance in the test operations.

REFERENCES

(1) Hung, T., C., Shai, T., Y., and Wang, S., K., 1997, "A Review of Organic Rankine Cycles (ORCs) for the Recovery of Low-Grade Waste Heat", *Energy*, 22(7), pp.661-667

(2) Inoue, N., Kaneko, A., Watanabe, H., Uchimura, T., and Irie, K., 2007, "Development of Electric Power Generation Unit Driven by Waste Heat (Study on Working Fluids and Expansion Turbine)", *Proceedings of GT2007 ASME Turbo Expo,* GT2007-27749

(3) Nakano, S., Kishibe, T., Inoue, T., and Shiraiwa, H., 2009, "An Advanced Microturbine System with Water-lubricated Bearings", *International Journal of Rotating Machinery*, Volume 2009, Article ID 71807

(4) Nakano, S., Tsubouchi, K., Shiraiwa, H., Hayashi, K., Yamada, H., 2010, "A 150kW Radial Inflow Steam Turbine System for the Bottoming Cycle of Reciprocating Engines", *ASME Turbo Expo,* GT2010-23231

(5) Balje, O., E., 1981, "*Turbomachines – A Guide to Design, Selection, and Theory"*, John Wiley & Sons, Inc., New York

(6) Perera, S., Dubitsky, O., 2006, "Application of the Concepts NREC agile engineering design system to steam turbines", *Turbomachinery Society of Japan*

(7) Dawes, N. W., 1988, Development of a 3D Navier Stokes Solver for Application to All Types of Turbomachinery, ASME Paper No.88-GT-70

(8) Nakano, S., Kishibe, T., Araki, H., Yagi, M., Tsubouchi, K., Ichinose, M., Hayasaka, Y. Sasaki, M., et al., 2007, "Development of a 150 kW microturbine system which applies the humid air turbine cycle", *ASME Turbo Expo* GT-2007-28192

(9) Hesler, S., and Segawa, K., 2001, "Benchmark testing of a low pressure steam wetness measurement probe in a model test turbine", *7th ERPI Steam Turbine/Generator Workshop and Vendor Exposition*, 20-23